Conference materials
UDC 539.421
DOI: https://doi.org/10.18721/JPM.161.110

Specific features of defect structure of a quartz single crystal at early stages of deformation

E.E. Damaskinskaya [1]✉, V.L. Hilarov [1], Yu.G. Nosov [1], K.M. Podurets [2], A.A. Kaloyan [2], D.V. Korost [3], K.A. Damaskinskii [4]

[1] Ioffe Institute, St. Petersburg, Russia;
[2] NRC Kurchatov Institute, Moscow, Russia;
[3] Lomonosov Moscow State University, Moscow, Russia;
[4] Peter the Great St. Petersburg Polytechnic University, St. Petersburg, Russia
✉ Kat.Dama@mail.ioffe.ru

Abstract. The paper is concerned with studies of the fracture process in a synthetic quartz single crystal under uniaxial compression at early stages of deformation by three independent techniques, i.e., acoustic emission, X-ray computed tomography and topography using a synchrotron radiation source. The most intense crack formation was observed in the region of higher internal deformations in the original crystal which were detected by topography. The energy of acoustic emission signals and the volume of the defects formed have been found to be linearly related. This result is of practical significance, since it allows estimation of sizes of fracture regions *in situ* merely by analyzing acoustic emission data in the cases, when other control techniques are inapplicable (for example, during the operation of industrial facilities).

Keywords: acoustic emission, X-ray computed tomography, synchrotron radiation topography (X-ray diffraction imaging), quartz single crystal, defects volume

Funding: This work was performed within the framework of the State assignment of the Ioffe Institute (0040-2014-0008).

Citation: Damaskinskaya E.E., Hilarov V.L., Nosov Yu.G., Podurets K.M., Kaloyan A.A., Korost D.V., Damaskinskii K.A., Specific features of defect structure of a quartz single crystal at early stages of deformation, St. Petersburg State Polytechnical University Journal: Physics and Mathematics. 16 (1.1) (2023) 60–66. DOI: https://doi.org/10.18721/JPM.161.110

Материалы конференции
УДК 539.421
DOI: https://doi.org/10.18721/JPM.161.110

Особенности дефектной структуры монокристалла кварца, сформировавшейся на ранних этапах деформирования

Е.Е. Дамаскинская [1]✉, В.Л. Гиляров [1], Ю.Г. Носов [1], К.М. Подурец [2], А.А. Калоян [2], Д.В. Корост [3], К.А. Дамаскинский [4]

[1] Физико-технический институт им. А.Ф. Иоффе РАН, Санкт-Петербург, Россия;
[2] НИЦ «Курчатовский институт», Москва, Россия;
[3] Московский государственный университет им. М.В. Ломоносова, Москва, Россия;
[4] Санкт-Петербургский политехнический университет Петра Великого, Санкт-Петербург, Россия
✉ Kat.Dama@mail.ioffe.ru

Аннотация. С помощью трех независимых неразрушающих методов — акустической эмиссии, рентгеновской компьютерной томографии, топографии с использованием источника синхротронного излучения — проведено исследование процесса разрушения

в синтетическом монокристалле кварца при одноосном сжатии на ранних этапах деформирования. Наиболее интенсивное образование трещин наблюдалось в области повышенных внутренних деформаций в исходном кристалле, обнаруженной с помощью топографии. Установлена линейная зависимость между энергией сигналов акустической эмиссии и объемом образовавшихся дефектов. Данный результат имеет практическое значение, поскольку позволяет в дальнейшем оценивать размеры областей разрушения *in situ* только по анализу данных акустической эмиссии в тех случаях, когда применение других методов контроля невозможно (например, при эксплуатации промышленных объектов).

Ключевые слова: акустическая эмиссия, рентгеновская компьютерная томография, рентгеновская дифракционная топография, объем дефектов, монокристалл кварца

Финансирование: Работа выполнена в рамках Государственного задания ФТИ им. А.Ф. Иоффе «Проблемы физики прочности: процессы разрушения твердых тел, принципы упрочнения материалов и повышения динамической прочности материалов, создание трещиностойких, износостойких материалов, разработка технологий легкой прозрачной брони» (код темы [0040-2014-0008]).

Ссылка при цитировании: Дамаскинская Е.Е., Гиляров В.Л., Носов Ю.Г., Подурец К.М., Калоян А.А., Корост Д.В., Дамаскинский К.А., Особенности дефектной структуры монокристалла кварца, сформировавшейся на ранних этапах деформирования // Научно-технические ведомости СПбГПУ. Физико-математические науки. 2023. Т. 16. № 1.1. С. 60–66. DOI: https://doi.org/10.18721/ JPM.161/110

Introduction

The fracture process caused by the formation of single submicro- and micro-cracks and their further evolution up to a macro-crack under the action of mechanical stresses is still not fully understood. This is due to the complexity of the experimental observation of defects in the material bulk during deformation without violating the integrity of the object of study.

One of the techniques that make it possible to control material damage *in situ* is the recording of acoustic emission (AE) signals that accompany the formation and development of submicro-, micro-, and macrocracks [1, 2]. It has been shown that acoustic emission in quartz occurs under high pressures, at heating and phase transformations [3–6].

The goal of our study was to trace the evolution of defects in a synthetic quartz single crystal by using complementary techniques, i.e., acoustic emission (AE), computed microtomography (CT), and X-ray diffraction imaging (XDI) or topography.

Experimental

We used a synthetic Z-oriented quartz crystal grown by hydrothermal synthesis at the All Union Research Institute for the Synthesis of Mineral Raw Materials [7]. Cylindrical samples (d = 10 mm, h = 20–24 mm) were cut from the crystal perpendicular to the {0001} pinacoid faces, the sample axis was in the <0001> direction.

The samples were subjected to uniaxial quasi-static compression at a loading rate (displacement of loading plates) of 5 μm/min on an AGX-Plus electromechanical machine (Shimadzu, Japan, maximum force 30 tons). The force was applied parallel to the cylinder axis. The compression was carried out up to a force equal to 6 kN, which corresponded to 0.08 of F_{max} (F_{max} is the breaking load, determined in preliminary experiments). The sample was then kept under constant strain until the AE activity dropped to zero (Fig. 2).

Acoustic emission signals were recorded in real time during sample loading by using the Amsy-5 Vallen system (Germany). Two AE105A piezoelectric transducers (frequency range 450–1150 kHz) were mounted at the sample ends. The accuracy of determining the coordinates of the AE signals hypocenters was not poorer than 2 mm. Each AE signal was characterized by the emission time, source coordinate along the sample height, and energy. The details of the experiment were described earlier; see, for example, [8].

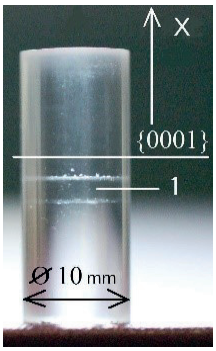

Fig. 1. Sample of a quartz single crystal (number 1 indicates the region of the sample where the seed is located; the white dots are the initial surfaces of the seed)

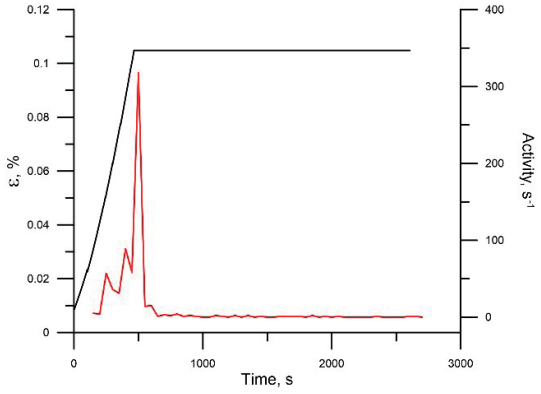

Fig. 2. Changes in strain (black line) and AE activity (red line) during the experiment

The study of the defects, characterized by a variation in the electron density of the material (in this case, pores or cracks), was performed by using X-ray computed microtomography (CT). Tomographic imaging before and after mechanical tests was carried out by a SkyScan 1172 tomograph (Bruker, Belgium) equipped with a Hamamatsu 100/250 microfocus X-ray tube and a detector (CCD — charge-coupled device 11-megapixel). For reconstruction the SkyScan's Nrecon software was used.

The selected sample size made it possible to achieve a spatial resolution of computed tomography of ~ 3 μm.

Tomographic imaging of the samples performed before mechanical testing revealed defects that were left from the seed surface. Figure 3 shows that the defects are located randomly inside the sample in the region with coordinates 11–14 mm in height. It was in this area that the seed was located (as can be seen in Figure 1). No defects such as cracks (discontinuities) were found outside the region of the seed plane.

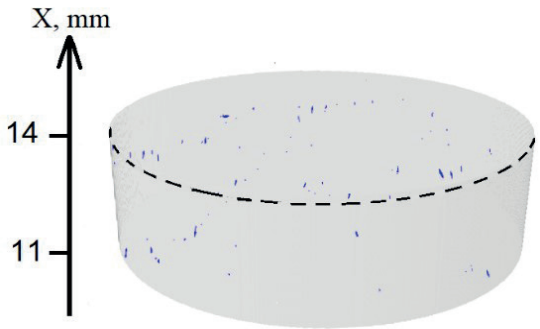

Fig. 3. Three-dimensional visualization of original defects (that were left from the seed) (blue objects)

To reveal the defects in the crystal structure and their aggregates, which did not affect the material density, but caused internal stresses, X-ray topography (XDI) was used. XDI made it possible to obtain an image of long-range strain fields in the form of a change in diffracted beam intensity (due to extinction contrast) [9]. Extinction contrast is a contrast, caused by local changes in the degree of crystal perfection.

Topographic studies were carried out at station "Median" of the Kurchatov specialized source of synchrotron radiation "KISI-Kurchatov". Images (topographs) were recorded by using a two-coordinate detector based on a 4008 × 2672 CCD matrix, a GdOS:Tb scintillator, with a pixel size of 8.9 μm. For image processing the ImageJ software was used [10].

Results and Discussion

The distribution of AE signal hypocenters along the sample height (Fig. 4) shows that the largest number of sources (in 7–10 times more than in other areas) is present in the 16–20 mm region. This implies that the most intense defect formation occurs in this region.

According to the data, described earlier in Section 2, there are no defects, associated with the seed in this region. A tomographic survey of the loaded specimen showed that the crack (black surface in Figure 5, *a*) was formed outside the original defects (red objects in Figure 5, *b*). Comparison of tomographic sections, obtained before and after loading, suggests that the initial defects at a given load level did not undergo any changes, i.e., neither germination of defects nor their closure was observed.

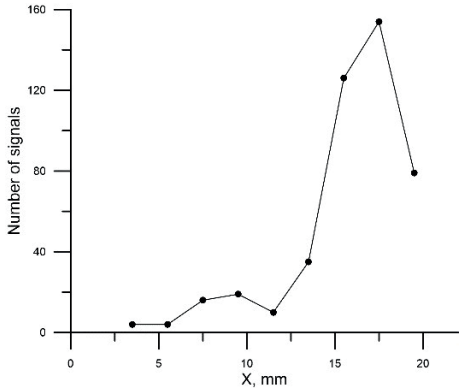

Fig. 4. Distribution of AE signals along the sample height

Figure 6 shows the change in the volume of defects in 2 mm high layers, determined from the CT data by using the CTan software. The largest volume of defects was detected in the 16–20 mm region. It is in this area that the fracture has a branched structure, which is demonstrated by the tomographic slices (Fig. 5, *c*).

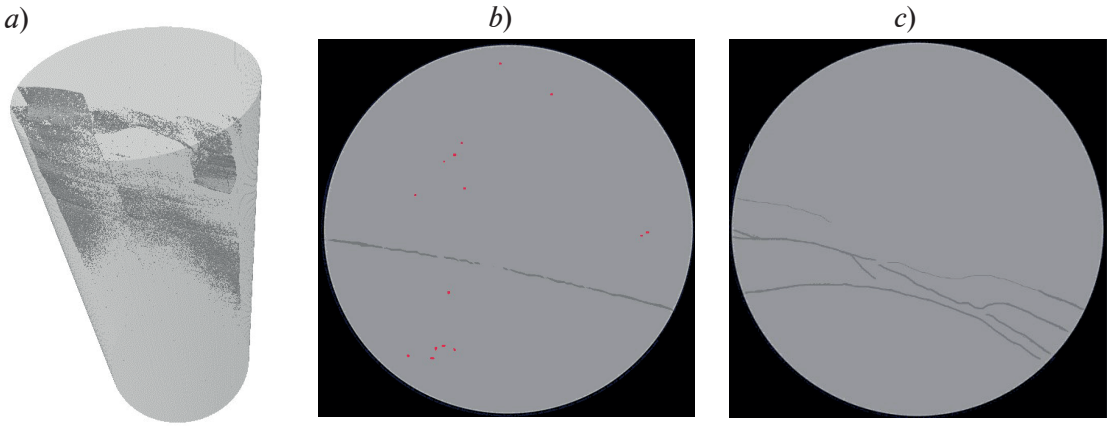

Fig 5. 3D visualization of the defect structure built from the X-ray tomography data using specialized CTan and CTvol softwares (*a*), and examples of tomographic sections: *b* — a slice of the area near the seed (the original defects are in red, the crack is in black); *c* — slice of the area with the most branched crack (black lines) far from the seed

A correlation between the mean signal energy AE and the volume of defects (Fig. 7) has been established. The dependence is approximated by a linear function (determination coefficient $R^2 = 0.89$). This result allows estimation of the volume of defects from the AE signals parameters.

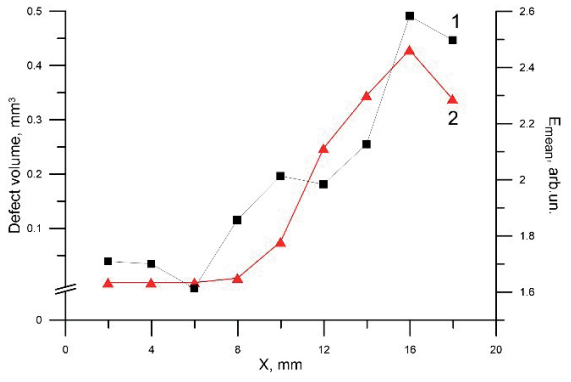

Fig. 6. Variations in the mean signal energy AE (gray curve 1) and defect volume (red curve 2) along the coordinate (sample height)

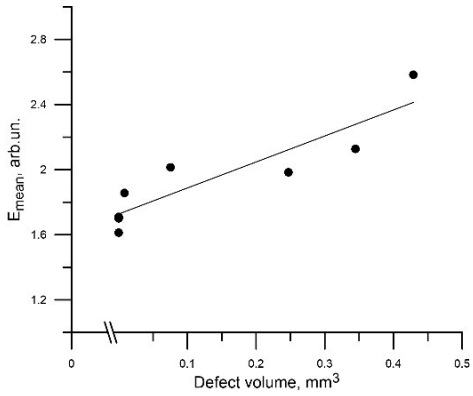

Fig. 7. Dependence of the mean signal energy AE on the volume of defects

X-ray topography revealed that the main "motif" of the defect structure was the presence of linear formations in the form of wavy fibers, extending along the sample height, i.e., in the direction of crystal growth (Fig. 8). The "fibers" are not an image of individual linear defects (dislocations), because in many cases they are observed to be broken, which is not typical of dislocations.

No elementary defects, such as dislocations, low-angle boundaries, etc., are detected on topographs. The observed imperfections are not discontinuities. It can be supposed that the fibrous structure is the manifestation of the assemblies of defects, mainly dislocations, the density of which is constant along the fiber and varies significantly in the transverse direction. There is the region in the crystal, in which the density of fibrous assemblies is higher as compared to the average density in the crystal (indicated by the arrow in Fig. 8, *a* and *b*).

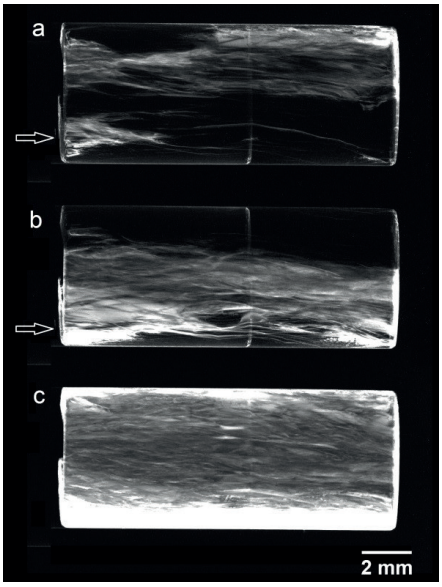

Fig. 8. Two topographs of the quartz crystal with an angular interval of 9.4", taken before application of a mechanical load (*a*, *b*), and a map of maximum intensity (*c*). A border of simultaneous reflection is observed in the middle of the image

Topographs of the quartz crystal were obtained after it was subjected to mechanical action. Analysis of the AE and CT data showed that the most developed crack (the largest amount of defects) was formed in the area with coordinates 16–20 mm. The topographs (Fig. 9) reveal a higher intensity in the same spatial region.

Thus, XDI allowed detection of a region of higher strains in the original sample. It is in this area that where the most intense cracking occurred after mechanical impacts, as evidenced by computed tomography.

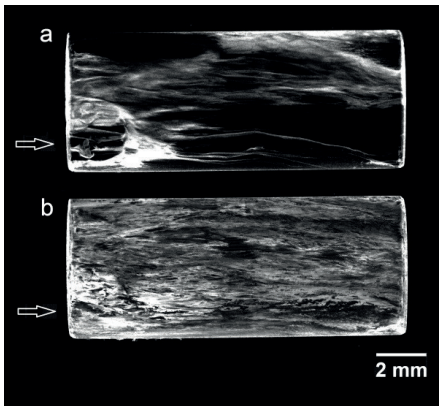

Fig. 9. A topograph of the quartz crystal, taken after application of a mechanical load (*a*), and a map of the rocking curve widths (*b*). The arrow indicates the region of fracture

The topographic pattern of fibers in the crystal bulk, obtained in our experiments, coincides with the pattern of structural defects in quartz, i.e, striations caused by assemblies of growth dislocations, which has been repeatedly described [7, 11]. The formation of cracks was observed in the region of higher densities of striae (fibrous formations) suggests that the primary structural defect, which gives rise to the formation of cracks under loading, are "bundle-like" dislocation clusters along the striae boundaries.

Conclusion

The accumulation of defects in a synthetic single crystal of quartz under uniaxial compression at early stages of deformation has been studied. A simultaneous application of three independent non-destructive techniques — acoustic emission, X-ray computed tomography, and the topography using a synchrotron radiation source — has given a more complete information on the development of fracture.

XDI allowed detection of the region of higher internal deformations in the original crystal.

Computed tomography visualized the cracks that were formed after load application and gave the data on the shape, size and volume of defects.

Analysis of parameters of acoustic emission signals allowed identification of the spatial region of the sample, in which defect formation was most intense.

Thus, the results obtained with the three techniques are consistent with each other and allowed detection of the region of the most intense defect formation in the sample bulk, and, what is especially important, allowed comparison of the parameters of the AE signals with those of the defects.

REFERENCES

1. **Xinglin Lei, Shengli Ma.,** Laboratory acoustic emission study for earthquake generation process, Earthquake Science. 27 (2014) 627–646.

2. **Voznesenskii A.S., Krasilov M.N., Kutkin Ya.O., Tavostin M.N., and Osipov Yu.V.,** Features of interrelations between acoustic quality factor and strength of rock salt during fatigue cyclic loadings, International Journal of Fatigue. 97 (2017) 70–78.

3. **Schmidt-Mumm A.,** Low frequency acoustic emission from quartz upon heating from 90 to 610 °C, Physics and Chemistry of Minerals. 17 (1991) 545–553.

4. **Glover P.W.J., Baud P., Darot M., Meredith P.G., Boon S.A., LeRavalec M., Zoussi S., Reuschlé T.,** α/β phase transition in quartz monitored using acoustic emissions, Geophysical Journal International. 120(3) (1995) 775–782.

5. **Gasc J., Schubnel A., Brunet F., Guillon S., Mueller H.-J., Lathe C.,** Simultaneous acoustic emissions monitoring and synchrotron X-ray diffraction at high pressure and temperature: Calibration and application to serpentinite dehydration, Physics of the Earth and Planetary Interiors. 189 (3–4) (2011) 121–133.

6. **Vettegren` V.I., Kuksenko V.S., and Shcherbakov I. P.,** Dynamics of fractoluminescence, and electromagnetic, and acoustic emission upon an impact against the marble surface, Technical Physics. 58 (1) (2013) 136–139.

7. **Dorogovin B.A. ed, et al.,** Sintez mineralov, Vol. 1 (2000). VNIISIMS, 2000 (in Russian).

8. **Damaskinskaya E.E., Hilarov V.L., Panteleev I.A., Gafurova D.R., and Frolov D.I.,** Statistical regularities of formation of a main crack in a structurally inhomogeneous material under various deformation conditions, Physics of the Solid State. 60(9) (2018) 1821–1826.

9. **Shul'pina I.L., Prokhorov I.A.,** X-ray diffraction topography for materials science, Crystallography Reports. 57 (2012) 661–669.

10. **Schneider C.A., Rasband W.S., Eliceiri K.W.,** NIH image to ImageJ: 25 years of image analysis, Nature Methods. 9 (7) (2012) 671–675.

11. **Kleshchev G.V., Kabanovich I.V., Chernyi L.N.,** On the nature of the optical inhomogeneity of quartz, Doklady AN SSSR. 174 (3) (1967) 585–586.

THE AUTHORS

DAMASKINSKAYA Ekaterina E.
Kat.Dama@mail.ioffe.ru
ORCID: 0000-0001-6328-0917

HILAROV Vladimir L.
Vladimir.Hilarov@mail.ioffe.ru
ORCID: 0000-0002-9211-6144

NOSOV Yurii G.
yu.nosov@mail.ioffe.ru

PODURETS Konstantin M.
Podurets_KM@nrcki.ru
ORCID: 0000-0003-2215-3692

KALOYAN Aleksandr A.
alexander.kaloyan@gmail.com

KOROST Dmitrii V.
dkorost@mail.ru
ORCID: 0000-0001-8957-6871

DAMASKINSKII Konstantin A.
damaskinsk@mail.ru
ORCID: 0000-0002-6692-2644

Received 13.10.2022. Approved after reviewing 08.11.2022. Accepted 08.11.2022.